NREL/TP-442-20164 • UC Category: 1211 • DE96000469

The Evaluation of a Turbulent Loads Characterization System

Neil D. Kelley
H. Edward McKenna

Prepared for
Fifteenth ASME
Wind Energy Symposium
January 28-February 2, 1996

National Renewable Energy Laboratory
1617 Cole Boulevard
Golden, Colorado 80401-3393
A national laboratory of the U.S. Department of Energy
Managed by Midwest Research Institute
for the U.S. Department of Energy
under contract No. DE-AC36-83CH10093

Prepared under Task No. WE514430

Available to DOE and DOE contractors from:
Office of Scientific and Technical Information (OSTI)
P.O. Box 62
Oak Ridge, TN 37831
Prices available by calling (615) 576-8401

Available to the public from:
National Technical Information Service (NTIS)
U.S. Department of Commerce
5285 Port Royal Road
Springfield, VA 22161
(703) 487-4650

17th ASME Wind Energy Symposium
January 29 - February 1996
Houston, Texas

THE EVALUATION OF A TURBULENT LOADS CHARACTERIZATION SYSTEM

Neil D. Kelley
H. Edward McKenna
National Wind Technology Center
National Renewable Energy Laboratory
Golden, Colorado 80401
Phone: 303-384-6923
Fax: 303-384-6901
E-mail: neil_kelley@nrel.gov

ABSTRACT

In this paper we discuss an on-line turbulent load characterization system that has been designed to acquire loading spectra from turbines of the same design operating in several different environments and from different turbine designs operating in the same environment. This system simultaneously measures the rainflow-counted alternating and mean loading spectra and the hub-height turbulent mean shearing stress and atmospheric stability associated with the turbulent inflow. We discuss the theory behind the measurement configuration and the results of *proof-of-concept* testing recently performed at the National Wind Technology Center (NWTC) using a Bergey EXCEL-S 10-kW wind turbine.

The on-line approach to characterizing the load spectra and the inflow turbulent scaling parameter produces results that are consistent with other measurements. The on-line approximation of the turbulent shear stress or friction velocity u_* also is considered adequate. The system can be used to characterize turbulence loads during turbine deployment in a wide variety of environments. Using the WISPER protocol, we found that a wide-range, variable-speed turbine will accumulate a larger number of stress cycles in the *low-cycle, high-amplitude (LCHA)* region when compared with a constant speed rotor under similar inflow conditions.

INTRODUCTION

In a previous study (Kelley, 1994b), we showed that the most damaging fatigue loads occur as a result of turbine rotors encountering turbulent regions in the inflow that have a distinct coherent or phase-specific structure. We also found that the majority of the fatigue damage to wind turbine blades made of composite material occurs in what we have called the *low-cycle, high-amplitude* or *LCHA* region (Kelley 1994a, Sutherland and Kelley 1995). The alternating load distributions in the LCHA region (with return rates of 100 cycles per hour or less) can be described by a decaying exponential distribution for all load parameters except the blade edgewise root moments. For this latter parameter, an extreme value distribution is appropriate. We also have shown (Kelley 1994a, 1995) that the shape parameters associated with the LCHA spectral distributions have a high degree of correlation with the hub-height mean turbulent shearing stress and static stability of the inflow. Ideally, we would like to acquire a range of statistically significant loading spectra and the corresponding inflow information from a turbine of identical design operating in number of different environments and different designs in the same environment. Such an activity would produce an extremely large volume of data to be processed and analyzed if conventional time-series recording is used.

In the past, the correlations between the decay rates of the LCHA region load spectra and the inflow parameters were determined from multi-channel time series data collected in the field and then post-processed. This approach, while necessary, can be very time consuming if a very large number of data records are collected at high sampling rates. With modern data acquisition equipment, it is possible to collect individual load spectra employing on-line rainflow cycle counting thereby passing the need for transferring and storing the actual load histories. It is possible to not only collect the load spectra on-line but the inflow correlating parameters as well. The volume of information acquired can be reduced to the essentials. Using this method, it is certainly feasible to collect and analyze the large data volume associated with the multi-turbine and multi-location measurements discussed above. This paper presents our approach to doing just that. We use an on-line system in which the load spectra from a 10-minute period are combined with the important statistical inflow parameters into a single, small data record for analysis. The system was evaluated using a Bergey EXCEL-S, 10-kW wind turbine installed on a 30.5-m (100-ft) tower at the National Wind Technology Center (NWTC). We compare our results using this technique with previous measurements taken in and near a multi-row wind park.

In past studies, we have used a protocol based on the derivation of the WISPER Reference Load Spectrum (Ten Have 1993) to compare characteristic loading environments (Kelley 1995, Sutherland and Kelley 1995). In this paper, we apply the WISPER protocol to our on-line measurement results gathered from the EXCEL-S turbine installed at the NWTC. We then compare these results with those from a multi-row wind park in San Gorgonio Pass, California and the WISPER itself (northern European conditions).

ON-LINE LOADS CHARACTERIZATION SYSTEM OVERVIEW

The loads characterization system consists of three major subsystems: the load measurements on the turbine, the inflow measurements, and the control/processing computer (PC). The loads subsystem consists of strain gages to measure the root flapping, torsion, and edgewise bending moments on one of the turbine blades and an integrated, microprocessor-based data acquisition unit that combines strain signal processing, low-pass filtering, quantization, and rainflow cycle counting. The inflow subsystem incorporates sensors or sensing systems and microprocessor-based data acquisition units to provide on-line, statistical measures of the inflow wind field and thermodynamic variables needed to characterize the turbulence and static stability. The PC is responsible for communicating control commands and data transfers between the turbine and inflow measurement subsystems. It also is responsible for error checking the acquired data, performing necessary derivative computations, and combining the results into a single, time-marked data record. Figure 1 schematically summarizes the system elements and parametric flow.

Loads Measurement

The heart of the turbine loads measurement system is a very rugged SoMat® Model 2100 Field Computer. The Model 2100, constructed around either a Hitachi/Zilog® HD64180Z or Z80180 microprocessor, is made up of a series of individual modules configured for a specific application. For this study, the Model 2100 configuration consisted of: the processor and memory modules, three programmable Butterworth low-pass filter modules, three strain gage bridge/quantizer modules, and two communications modules. In addition to the Model 2100 Field Computer, communications with the controller/processor PC were made via a SoMat Wireless Data Link®. This link, which uses 900-MHz Spread Spectrum radio technology, allows two-way communications between the Field Computer mounted on the turbine hub and the ground-based PC at a rate of 19.2 Kbaud.

One blade of the EXCEL-S turbine was instrumented for root flapwise, torsional, and edgewise bending relative to a position 0.2 m from the hub. The strain signals were passed through low-pass filters with a 4-pole Butterworth characteristic and a breakpoint frequency of 400 Hz before being quantized to an eight-bit resolution. Because of the high rotational speeds of the EXCEL-S turbine (which can exceed 350 rpm), the load signals were sampled at a rate of 600 per second. An examination of frequency spectra derived from unfiltered load histories showed no evidence of significant signal energy in excess of the Nyquist frequency of 300 Hz.

The Model 2100 Field Computer was programmed using SoMat TCS® software to collect and process a 10-minute record upon receiving a start command from the PC. Each of the strain signals was rainflow-cycle counted on-line, producing a 64x64 range/mean matrix with all open or half cycles being closed at the end of the period. After the collection period and at the command of the PC, the matrix for each load parameter was uploaded to the PC via the radio link.

Inflow Measurement Subsystem

The purpose of the inflow measurement subsystem is to provide statistical measures of important scaling parameters acquired over the same 10-minute period that the blade bending loads are being rainflow-counted on the turbine. The required measurements included the mean hub-height horizontal wind speed (U), standard deviation (σ), the hub-height friction velocity (u_*), and the gradient Richardson number stability parameter (Ri). In addition to the meteorological parameters, the number of blade rotations also was included so the WISPER protocol could be applied to the data set.

Normally, measurement of the friction velocity ($u_* = \left(\overline{-u'w'}\right)^{1/2}$) is performed off-line by removing the means (leaving only the fluctuating part and indicated by a prime) of the longitudinal or along-the-wind (u) and vertical wind components (w) from the time series and then calculating the product ($u'w'$). In order to achieve an on-line estimate of u_*, we used the approximation $(-u'w')^{1/2} \approx (-U'w')^{1/2}$ for which the error normally does not exceed more than 2% for wind speeds of interest in wind energy conversion. A Kaijo-Denki Model DA-600 sonic anemometer was used as the hub-height wind speed measurement. This instrument was programmed to provide measurements of U and w at a rate of 20 per second. To obtain the zero mean quantities U' and w', we removed all signal contributions with periods longer than 2 minutes by passing them through 4-pole Butterworth high-pass electronic filters. The high-passed signals then were fed to a Campbell Scientific 21X scientific data logger that was programmed to compute the $U'w'$ covariance on-line at a sampling rate of 20 per second. This data logger also was used to compute the mean of the horizontal wind speed, its standard deviation, and the peak gust observed during the recording period.

Our previous work (Kelley 1994a, 1994b) has shown that the LCHA range loads are produced by coherent structures of turbulence manifested by large values of the instantaneous shear stresses $u'w'$, $u'v'$, and $v'w'$. Earlier measurements upstream and downstream of a large multi-row wind park in the San Gorgonio Pass of California showed that the contributions to these structures occurred at time scales less than 1 minute. Figure 2

plots the approximately normal distributions of the instantaneous u'w' shearing stress component integral time scales I_T ($I_T = \int_o^T R(\tau)d\tau$ where $R(\tau)$ is the autocorrelation of the instantaneous u'w' shearing stress and T is the record length) for these two locations. The I_T represents the longest period of time in which the signal is correlated with itself. The distribution associated with the location upstream of the wind park has a characteristic (median) integral time scale of about 30 s and the downstream station about three-quarters of that, or 22 s. The values go to zero for periods longer than 60 s for both locations. Thus, we believe we are being conservative in passing shear stress fluctuations with periods as long as 2 minutes. We are confident that we are adequately capturing the contributions to the U'w' covariance with our on-line approximation.

As is shown in Figure 1, a second 21X data logger was used to collect and partially process the meteorological variables required to calculate the gradient Richardson number stability parameter

$$Ri = \left(\bar{\theta} / g\right)(\partial\theta / \partial z) / (\partial U / \partial z)^2$$

where $\theta = T(1000 / p)^{.286}$, p is the barometric pressure in hPa, T is the absolute air temperature (K), g is the gravity acceleration (m/s^2), and z is the height in meters. The Richardson number represents the ratio of turbulence generation by buoyancy to shear forces and is an important turbulence scaling parameter. This logger, sampling at a rate of 1/s, provided 10-minute means of the wind shear, temperature difference between 3 and 37 m (the top of the turbine rotor), 3-m temperature, barometric pressure, and the 37-m wind speed and direction. It also was used to summarize the number of rotor revolutions from the turbine.

Control/Processing Computer Subsystem

The computer program cycled through the data collection sequence, which included initializing the hub-mounted Field Computer and the two 21X data loggers and returning 10 minutes later to upload the stored results. These reports were then error-checked, and the values of u_* and Ri were calculated. The inflow meteorological data were combined with the rotor revolutions and the three rainflow matrices (as is indicated in the lower left-hand portion of Figure 1) and written into a single disk file with the time-of-day, error codes, and system information. When operating continuously, the overall duty cycle was approximately 13.5 minutes for each 10-minute data record collected. Also, when the wind direction was within 15 degrees of being directly downwind of the meteorological tower, an error code was substituted for the value of u_* so that it would not be influenced by shedding from the support tower members and the turbine wake.

SYSTEM EVALUATION AND RESULTS

A total of 1001 data records were collected between mid-April and mid-June 1995. Initial difficulties in programming the output of the sonic anemometer and the loss of data that fell within the excluded wind direction range resulted in only 525 of these records containing a useful u_* value. While the majority of the observed mean wind speeds were less than 5 m/s, we did experience a wide range of inflow conditions and wind speeds. Flow conditions included winds coming off the rolling terrain to the north through southwest and from the Rocky Mountain foothills to the west of the NWTC. We acquired several records that had a mean wind speed more than 17 m/s. In this section, we discuss the results in comparison to similar measurements taken in and near a multi-row wind park in San Gorgonio Pass, California.

To reduce the scatter seen in the individual 10-minute records, we classified the available population with respect to mean wind speed and Richardson number stability. The population was stratified into seven wind speed and five stability classifications. We then calculated an array of descriptive statistics of the parameters of interest for each of these 12 classifications.

Evaluation of On-Line Approximation of u_*

The upwind fetch associated with the measurements taken in the San Gorgonio Pass is very similar to that seen at the NWTC. The terrain upstream of this site consisted of both complex (canyons and foothills) and smooth or rolling elements, but contained no wind turbines. Therefore we would expect the variation in the value of u_* with mean hub-height wind speed (U) to be similar for both sites. We would not necessarily expect a similar variation downwind of a 41-row wind park. Figure 3 summarizes these three variations of u_* versus U. As can be seen, u_* varies linearly with wind speed at the San Gorgonio upstream station. The on-line, approximate values measured at the NWTC also exhibit a linear trend but deviate from the San Gorgonio data at low wind speeds. Neither the upstream San Gorgonio data nor the NWTC data follow the non-linear variation seen downstream of the wind park.

The variation of u_* with U over homogeneous terrain is known to follow $u_* = 0.4U / [\ln(z / z_o) - \psi_m]$, where z_o is the surface roughness length, and ψ_m is the *diabatic* term that is positive for unstable flows, negative for stable flows, and zero for neutral conditions (Panofsky and Dutton 1984). For a fixed height above the ground, constant roughness, and neutral conditions, this relationship indicates that u_* varies linearly with wind speed. Increasing the value of z_o in neutral conditions increases the rate of change of u_* with U. Similarly, with a constant surface roughness, increasing the stability of the flow increases u_* with U and vice versa.

We believe the deviation of the NWTC values of u_* from those of the San Gorgonio upwind location in Figure 3 is due to the predominance of stable, easterly flows over rolling terrain (lower surface roughness values) in the data set. As the wind

speed increases above 10 m/s, the NWTC data asymptotically approach the San Gorgonio values and trend line. At higher wind speeds, the stability approaches neutral and the influence of the diabatic term diminishes. Based on these results, we conclude that our on-line approximation of u_* is adequate and consistent with what would be expected at the higher wind speeds where turbines are most sensitive to turbulence-induced loads. Had the measurements for both sites been taken at the same elevation, we believe values would be even closer.

In analyzing the San Gorgonio data from within the wind park, we noted a strong correlation between u_* and the Ri in near-neutral flow conditions (Kelley 1994a). We believe this to be a consequence of the dynamic instability present in the internal wind park flows. Under such conditions, small-scale perturbations can grow exponentially with time. This can lead to the development of non-linear flow phenomena such as Kelvin-Helmholtz instabilities that produce strong, transient shears and coherent turbulent structures. We compare the variation of u_* with Ri for a narrow range about neutral in Figure 4. A similar behavior is apparent at the NWTC and within the multi-row wind park in San Gorgonio, though the values of u_* are much higher for the latter location. This suggests that the underlying dynamics of this peaking behavior are similar if not the same for both sites. It also supports our conclusion that the on-line approach does indeed capture the important aspects of the inflow.

LCHA Load Range Inflow Correlation Comparisons

Kelley (1994a) showed that the LCHA range load spectra (scaled in cycles/hr) of all turbine load parameters except the root edgewise bending could be fitted by a decaying exponential distribution, $N = 100 \exp(-M_{p\text{-}p}/\beta_1)$, where β_1 is the distribution shape parameter, $1/\beta_1$ is the rate or slope, and $M_{p\text{-}p}$ is the peak-to-peak (p-p) bending moment. For the root edgewise bending moment, a Type I (Gumbel) extreme value distribution was found to best fit the observations. This distribution is given by $N = \gamma_o \exp\{-\exp[-((M_{p\text{-}p}-\gamma_1)/\gamma_2)]-[((M_{p\text{-}p}-\gamma_1)/\gamma_2)] + 1\}$, where γ_o is the scale or amplitude parameter, γ_1 is the position parameter and corresponds to the once-per-revolution gravity or 1-P load peak, and γ_2 is the width or shape parameter. These distributions are shown schematically in Figure 5. It is the parameters $1/\beta_1$ and γ_2 that we have correlated with u_* and Ri.

The LCHA exponential distribution slope or rate ($1/\beta_1$) was determined for the root flapwise and torsional moments and the edgewise root moment extreme value distribution shape parameter γ_2 for each of the individual load spectra for which they could be defined. It was not always possible to establish a value for these parameters because a minimum of three data points in the LCHA Range were needed to fit the exponential distribution and four for the extreme value. Under very smooth flow conditions and/or low wind speeds, this condition was often not met, particularly for the torsional bending spectra. As a result, fewer than the maximum number of records available are included in each of the bending moment sub-populations.

The relationships between the LCHA range shape parameters for the flap and edgewise root moments ($1/\beta_1$, γ_2) and (1) the inflow u_* and Ri parameters for the Micon 65/13 turbines in the multi-row San Gorgonio wind park and (2) the EXCEL-S at the NWTC are plotted in Figures 6a and 6b, respectively. The data from the Micon 65's using the NREL S-series airfoils and the original AeroStar blades have been combined on these diagrams. The trend line of the u_* - Ri relationship from Figure 4 also has been included for reference. It is clear from these plots that, while strong responses are associated with just slightly stable conditions in both locations, the multi-row wind park is much more severe. The Ri range of a resonant-type response for the NWTC EXCEL-S appears to be much narrower than that of the wind park. An analysis-of-variance analysis (ANOVA) of the EXCEL-S flap and edgewise moment data showed that the shape parameters were about equally sensitive to u_* and the standard deviation, σ, and much more weakly correlated with Ri. As was the case at San Gorgonio, there was no significant correlation with the turbulence intensity, σ/U.

An ANOVA of the root torsional bending data indicated that only the hub-height mean wind speed was significantly correlated with the LCHA range exponential slope. Figure 7 plots this relationship, which varies parabolically with wind speed.

COMPARISON VIA THE WISPER PROTOCOL

Kelley (1995) recently compared the service environments in northern Europewith those in the San Gorgonio wind park using the WISPER (Ten Have 1993) loading standard and its development protocol. Sutherland and Kelley (1995) took this a step further by using the service lifetime predictions based on the WISPER protocol to compare and contrast the two loading environments. The normalization scheme employed in the WISPER protocol allows such comparisons to be made between turbines of different designs and operating environments.

A Brief Synopsis of the WISPER Protocol

The WISPER reference-loading spectrum was developed by an international working group composed of thirteen different European research institutes and manufacturers (Ten Have 1993). The objective of the effort was to specify variable-amplitude (or spectral) test-loading histories that incorporate the major features seen in the root flapwise (out-of-plane) bending of horizontal-axis wind turbine (HAWT) blades. These features include exhibiting a spectral shape that is characteristic of the type of structure under test, while also providing the interactions thought to be important in such a stochastic environment. Great care was taken to ensure that the final loading spectra did not represent any particular turbine design or operating environment (i.e., no attempt was made to provide for a realistic time correlation). These features imply that the standard is to be used

for comparative purposes only. The WISPER protocol refers to the steps that were followed to arrive at the WISPER reference-loading spectrum.

The WISPER protocol is defined by eight load cases that are called "classes" or "operating modes." The first two modes are the loads for discrete events, specifically turbine start-up (Mode 1) and stopping (Mode 2). The six remaining classes, 3 through 8, are based on 10-minute load histories obtained during continuous operation of turbines over their operating wind speed range. Mode 3 contains representative data for mean wind speeds below 9 m/s. Modes 4 through 7 contain data for mean wind speeds of 9-11, 11-13, 13-15, and 15-17 m/s, respectively. Finally, Mode 8 describes the loads for mean wind speeds exceeding 17 m/s.

Turbine load range-mean matrices for Modes 3 through 8 are normalized (called normalized range [nrv] or mean values [nmv]) by the magnitude of the alternating load cycle occurring once per 1000 revolutions. Using this approach, six normalized load-cycle matrices are obtained-- one each for of the operating Modes (wind speed classes) 3 through 8). Because we are interested only in conditions during continuous operation, we have ignored the start-up and shutdown Modes 1 and 2. Finally, after discarding values less than 0.6 nrv to reduce the number of loading cycles, the normalized loading range is expressed by a series of discrete values called WISPER Levels. These test levels (which represent load p-p values in normalized space) range from 1 to 64, with a value of 25 representing the zero load condition. The total load spectrum is obtained by adding together the contribution of each loading spectrum from each wind class in proportion to the number of hours the turbine will operate in that class during a 2-month period. The hours of operation used in the original WISPER protocol are based on the long-term wind statistics from two different sites along the coast of northern Germany.

Application to the NWTC EXCEL-S Turbine

The WISPER protocol was applied to the 1001 10-minute root-flapwise loading spectra available. Table 1 summarizes the important parameters for each of the six operating wind speed classes (WISPER Modes 3-8). Because the EXCEL-S is a freewheeling, variable-speed machine, for comparative purposes it was necessary to increase the WISPER-specified rotational speed of 45 rpm to agree with the values in Table 1 for each wind speed class. This increased the number of alternating loads cycles in the WISPER spectrum in proportion to the increase in rpm for each wind speed class or operating mode. The normalized EXCEL-S spectrum is contrasted with the WISPER reference load spectrum in Figure 8 based on the WISPER-specified 2-month wind speed distribution. The figure shows that the EXCEL-S 2-month loading block would, in all probablity, be more damaging.

Figure 9 compares the variation in WISPER Level range size (normalized load p-p value) using the normalized range value (nrv) with the original WISPER and San Gorgonio distributions. It is apparent that the EXCEL-S curve behaves similarly to the WISPER (e.g., no stratification with operating mode or wind speed class), but has a much steeper slope. The San Gorgonio data, however, stratify with wind speed class, the slope increasing monotonically with increasing wind speed class. It is also interesting to note that the slopes of the San Gorgonio Modes (wind classes) 3 and 7 are almost coincident with those of the EXCEL-S.

INTERPRETATION

With respect to the slopes of the curves shown in Figure 9, we believe the steep curve associated with the EXCEL-S data taken at the NWTC is a consequence of the freewheeling, variable-speed operation of this turbine. Each of the nine turbines used to obtain baseline data for the WISPER reference standard operated at constant rotor speed as did the Micon 65's in the San Gorgonio wind park. The sharp increase in loads over a constant speed rotor is consistent with several factors, including the increase in dynamic pressure on the blades and the accompanying sensitivity to unsteady aerodynamic effects. McCroskey (1981) points out the enhanced sensitivity to leading edge stall phenomena for freestream Mach numbers more than 0.2. For the EXCEL-S, the blade tip Mach number can achieve a value of 0.4 or more at maximum power (~350 rpm) before furling is initiated. We noted distinct acoustical evidence that some form of unsteady loading was taking place during unfurled operation at this high rotational speed.

We maintain that the slopes representing the San Gorgonio wind park increase monotonically with wind speed class is a result of the non-linear increase in hub-height mean shear stress (u_*) with wind speed depicted in Figure 3. The large values of u_* represent highly coherent turbulent conditions. Tangler, et al. (1994) found that coherent turbulence was most important source of blade flapwise and low-speed shaft bending loads on the Micon 65. The lack of scatter in the data plotted for both the WISPER and the EXCEL-S indicates an insensitivity to wind speed class. We believe such a lack of scatter (or stratification with wind speed class) is a direct result of the linear behavior of u_* with increasing wind speed shown in Figure 3. We conclude that the larger number of alternating cycles in the high-loading tail of the EXCEL-S spectrum of Figure 8 is a consequence of the wide range of variable speed operation and not the characteristics of the turbulent inflow.

The slopes in Figure 9 and the behavior of the value of u_* versus wind speed in Figure 3 we hypothesize there may be only two classes of turbulent inflow important to wind turbine operations. These are internal wind park and non-wind park environments. We currently lack sufficient evidence to validate such a hypothesis. We do postulate, however, that the differentiating factor between the two classes lies in the behavior of u_* in slightly stable conditions, as exemplified in Figures 6a and 6b. This would suggest that the interaction between multiple turbine wakes and a dynamically unstable atmospheric boundary layer (Kelley 1994a) is the underlying

cause. Undoubtedly similar conditions can conceivably occur outside multi-row wind parks, but the question is how often and under what circumstances? It may therefore be appropriate to consider a third class of turbulent inflows in which strong, non-linear behavior occurs outside of a wind park. An example of such a situation would be a separating boundary layer flow near an escarpment.

CONCLUSIONS

Based on the results of this study, the on-line approach to characterizing load spectra and inflow turbulent scaling parameters produces results that are consistent with other measurements. The on-line approximation of the turbulent shear stress or friction velocity u_* is seen to be adequate. The system can be used to characterize turbulence loads on wind turbines installed in a wide variety of operating environments.

The results show that turbulent conditions within a multi-row wind park are significantly different from those seen even in relatively complex terrain. This suggests that perhaps only two or possibly three turbulent inflow descriptions may be needed for the evaluation of turbine fatigue lifetimes.

Application of the WISPER protocol to the data collected indicates that a variable speed turbine, particularly one with a wide operating range such as the EXCEL-S, will accumulate fatigue damage at a greater rate than an equivalent machine using a constant speed rotor.

FUTURE WORK

Future studies will involve exposing the on-line characterization system with an EXCEL-S turbine within the San Gorgonio wind park to determine if load stratification occurs with increasing WISPER wind speed class as was observed in turbines with constant speed rotors. We will attempt to validate or modify the postulate that only two or three inflow turbulence descriptions are necessary by repeating these measurements in various operating environments on turbines of varying design.

ACKNOWLEDGMENTS

This work has been supported by the U.S. Department of Energy under Contract DE-FC02-86CH10311. The authors wish to acknowledge the major contributions to the success of this project made by Bob Keller, Bill Gage, and Sherm West of Mountain Valley Energy and instrumentation engineer Doyle Selix. We also wish to thank Rich Osgood, Jerry Bianchi, and Jack Allread of NREL; Mike and Karl Bergey and Peter Huebner of Bergey Windpower; and John Poust of the SoMat Corporation for their support in this effort. We appreciate the benefits derived from discussions with Mike Robinson and Jim Tangler of NREL and Kevin Jackson of Dynamic Design.

REFERENCES

Kelley, N.D., 1994a, "The Identification of Inflow Fluid Dynamics Parameters That Can Be Used to Scale Fatigue Loading Spectra of Wind Turbine Structural Components," *Wind Energy 1994*, W. Musial, S. Hock, and D. Berg (eds), SED-Vol.15, ASME.

Kelley, N.D., 1994b, "Turbulence Descriptors for Scaling Fatigue Loading Spectra of Wind Turbine Structural Components," NREL/TP-442-7035, National Renewable Energy Laboratory, Golden, CO.

Kelley, N.D., 1995, "A Comparison of Measured Wind Park Load Histories with the WISPER and WISPERX Load Spectra," *Wind Energy 1995*, W. Musial, S. Hock, and D. Berg (eds), SED-Vol.16, ASME.

McCroskey, W.J., 1981, "The Phenomenon of Dynamic Stall," NASA TM-8124, NASA Ames Research Center, Moffet Field, CA.

Panofsky, H.A., and Dutton, J.A., 1984, *Atmospheric Turbulence*, John Wiley & Sons, New York, NY.

Sutherland, H.J. and Kelley, N.D., 1995, "Fatigue Damage Comparisons for Northern European and U.S. Wind Farm Loading Environments," *Proceedings WindPower '95*, American Wind Energy Association, Washington, DC.

Tangler, J., Kelley, N.D,. Jager, D., and Smith, B., 1994, "Measured Structural Loads for the Micon 65/13," *Wind Energy 1994*, W. Musial, S. Hock, and D. Berg (eds), SED-Vol.15, ASME.

Ten Have, A.A., 1993, "WISPER and WISPERX: A Summary Paper Describing Their Backgrounds, Derivation, and Statistics," *Wind Energy 1993*, S. Hock (ed), SED-Vol.14, ASME.

TABLE 1. EXCEL-S WISPER Protocol Data.

Wind Class (Operational Mode)	Number of 10-minute records	Hours	Mean Wind Speed (m/s)	Mean Rotor speed (rpm)	Class Normalizing Value [nrv] (Nm)
3	834	139.00	5.40	97.6	525
4	87	14.50	9.99	195.8	501
5	39	6.50	11.87	254.6	437
6	24	4.00	13.92	319.8	389
7	13	2.17	15.70	354.1	376
8	4	0.67	18.20	351.0	483

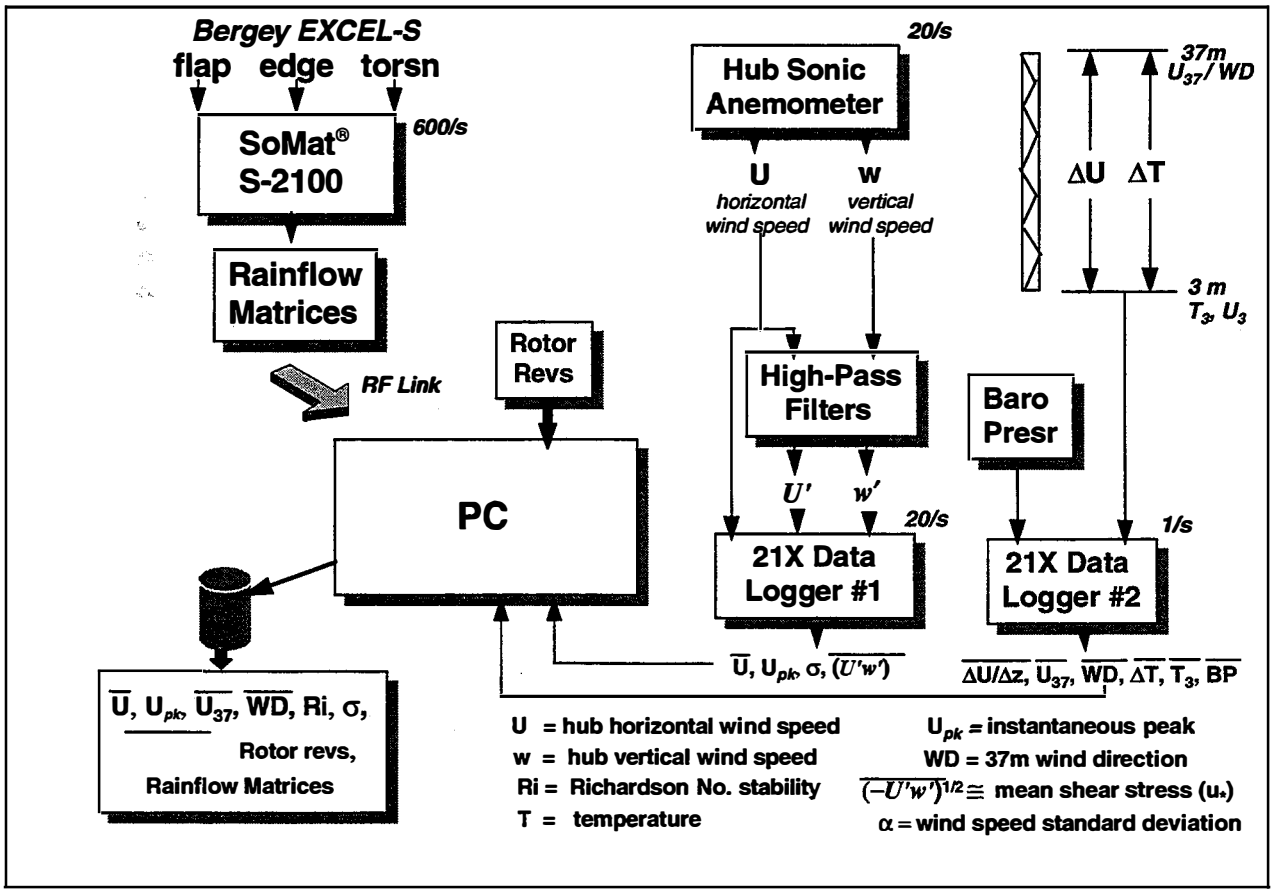

Figure 1. Schematic of Load Characterization System.

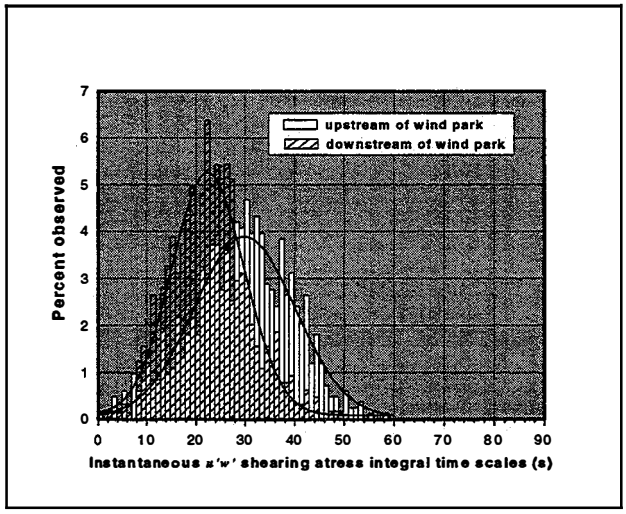

Figure 2. San Gorgonio Instantaneous u'w' Shearing Stress Integral Time Scale Distributions.

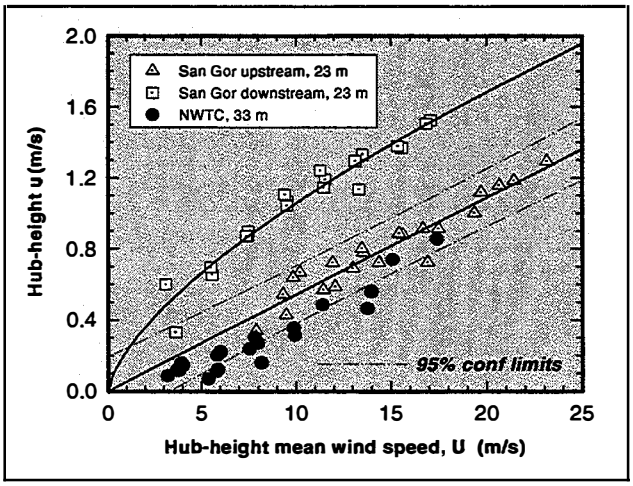

Figure 3. Comparison of U vs u∗ for the NWTC and San Gorgonio Sites.

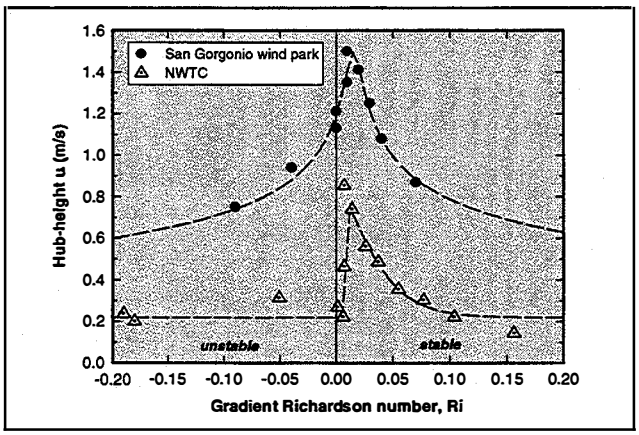

Figure 4. Ri vs u_* Behavior for the NWTC and San Gorgonio Sites.

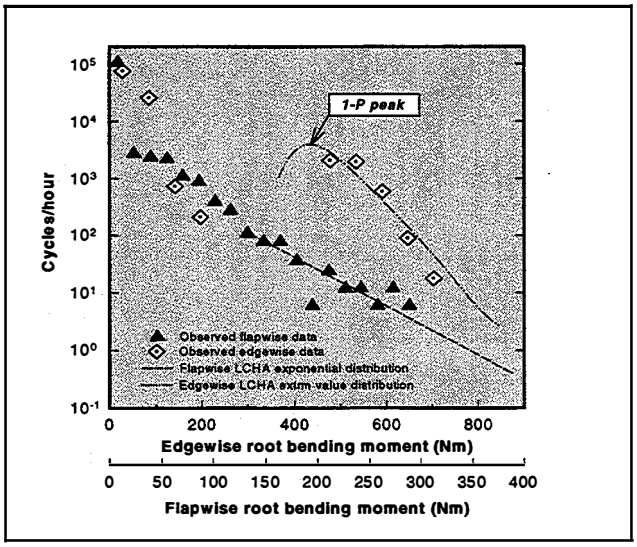

Figure 5. EXCEL-S LCHA Region Example.

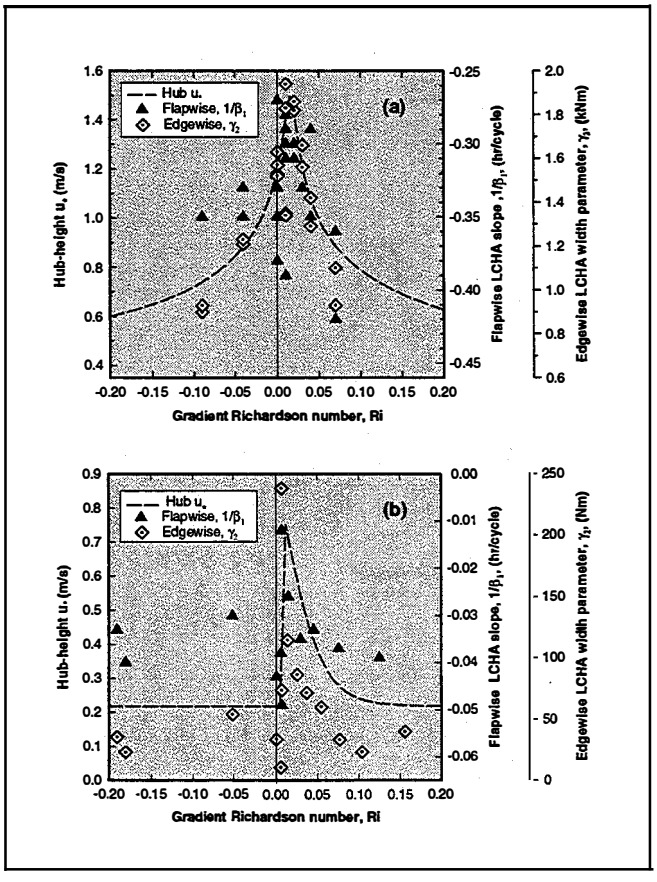

Figure 6. LCHA Range Sensitivities for: (a) San Gorgonio Micon 65; (b) NWTC EXCEL-S.

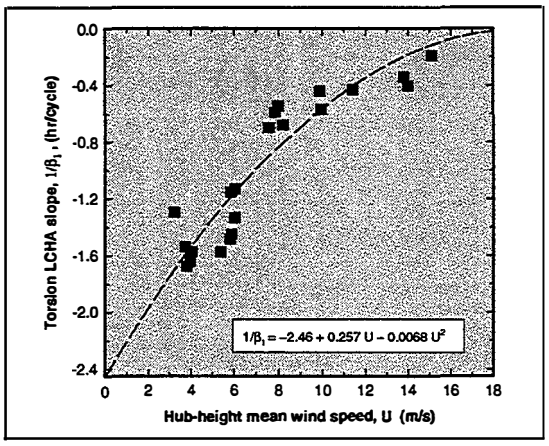

Figure 7. EXCEL-S LCHA Range Torsional Sensitivity.

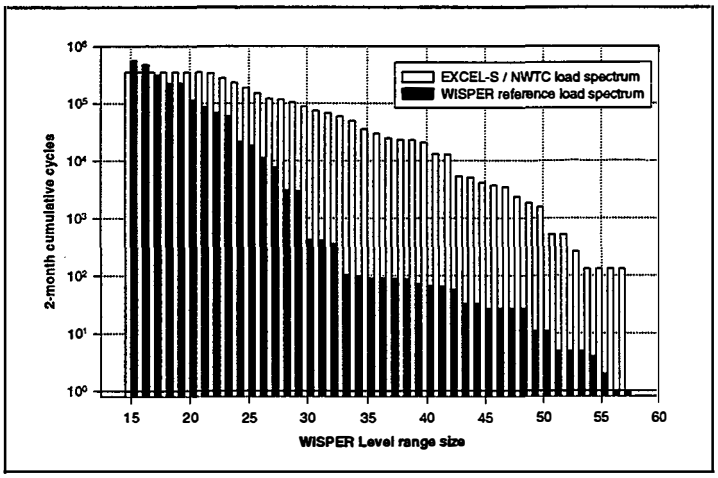

Figure 8. Comparison of EXCEL-S Normalized Load Spectrum Using WISPER Wind Speed Distribution.

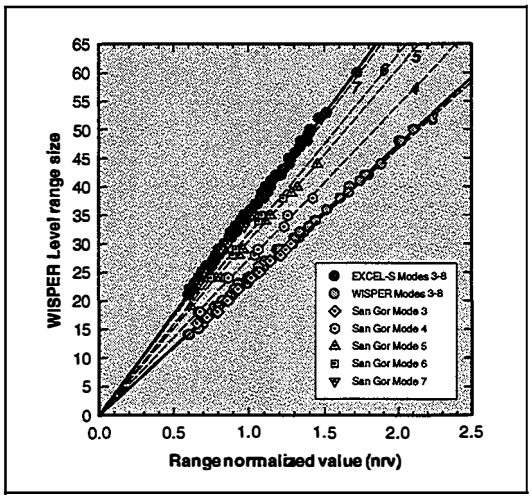

Figure 9. Comparison of WISPER Level Range Size vs Range Normalized Value.